On-Orbit Performance of the TRMM Mission Mode

Brent Robertson, Sam Placanica, Wendy Morgenstern
NASA Goddard Space Flight Center

Joseph A. Hashmall, Jonathan Glickman, Gregory Natanson
Computer Sciences Corporation

Contact: Brent Robertson
e-mail: brent.robertson@gsfc.nasa.gov
phone: (301) 286-6392

Abstract

This paper presents an overview of the Tropical Rainfall Measuring Mission (TRMM) Attitude Control System along with detailed in-flight performance results of the TRMM Mission Mode. TRMM is a joint mission between NASA and the National Space Development Agency of Japan designed to monitor and study tropical rainfall and the associated release of energy.   The TRMM spacecraft is an Earth-pointed, zero momentum bias satellite launched on November 27, 1997 from Tanegashima Space Center, Japan. Prior to calibration, the spacecraft attitude showed larger Sun sensor yaw updates than expected. This was traced to not just sensor misalignment but also to a misalignment between the two heads within each Sun sensor. In order to avoid alteration of the flight software, Sun sensor transfer function coefficients were determined to minimize the error due to head misalignment. This paper describes the design, on-orbit checkout, calibration and performance of the TRMM Mission Mode with respect to the mission level requirements.

TRMM Mission Overview

TRMM is a joint mission between NASA and the National Space Development Agency (NASDA) of Japan designed to monitor and study tropical rainfall and the associated release of energy shaping both weather and climate around the globe. TRMM is the first mission dedicated to measuring rainfall through five microwave and visible infrared sensors, including the first spaceborne rain radar. Launched to provide a validation for poorly known rainfall data sets generated by global climate models, TRMM has demonstrated its utility by reducing uncertainties in global rainfall measurements by a factor of two. A sample image taken by one of the TRMM instruments is shown in Figure 1.
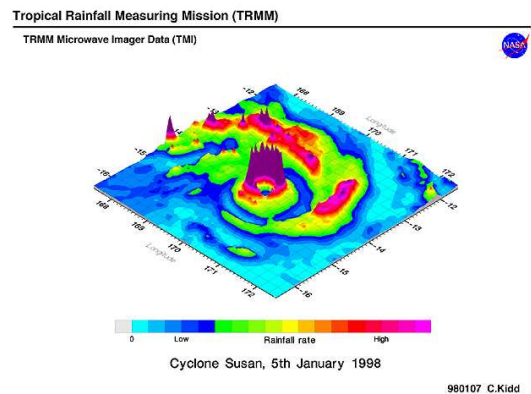

Figure 1: TRMM Science Image

The TRMM spacecraft, shown in Figure 2, was launched on the H-II Expendable Launch Vehicle on November 27, 1997 from Tanegashima Space Center, Japan. The spacecraft is three-axis stabilized, in a near circular 350 km orbit with inclination of 35°. At launch, the spacecraft had a mass of 3,523 kg including 903 kg of fuel and pressurant.
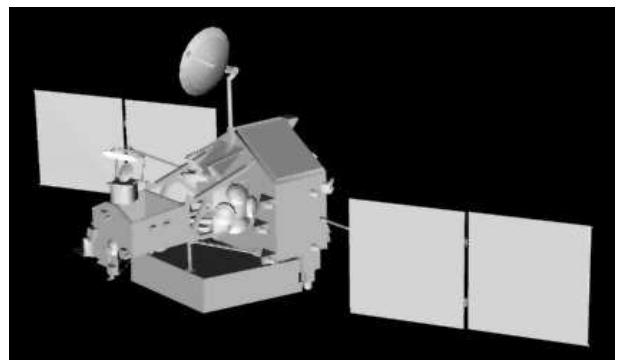

Figure 2: TRMM Spacecraft

TRMM Attitude Control System Design

The TRMM Attitude Control System (ACS) Mission Mode is required to maintain a nadir pointing attitude

with requirements shown in Table 1[1]. Since the science requirement did not specify either a geocentric or geodetic reference, for convenience the nadir reference was defined by the output of the chosen Earth Sensor Assembly (ESA). This resulted in a nadir reference (Z) defined by a horizon bisector of the CO_2 horizon of the Earth, so that spacecraft pointing is provided with respect to a quasi-geodetic position. Analysis shows that this reference frame is approximately 0.01^O from the geodetic frame with nominal ESA performance.

Table 1: ACS Mission Mode Pointing Requirements

Characteristic	Requirement (per axis)
Pointing Knowledge, on-board (3σ)	0.2^O
Pointing Accuracy (3σ)	0.4^O
Stability (peak to peak)	0.1^O over 1 sec

Due to an instrument thermal requirement that the +Y side of the spacecraft stay cold, the Mission Mode is required to operate in either a +X forward or –X forward orientation. The spacecraft is commanded to rotate 180° about nadir (yaw) every few weeks when the Sun crosses the orbit plane. Due to these yaw rotations, the spacecraft maintains an angle between the Sun and the spacecraft X-Z plane of between 0° and 58.4^O.

The TRMM ACS architecture is shown in Figure 3. The ACS is comprised of Attitude Control Electronics (ACE), an ESA, Digital Sun Sensors (DSS), Inertial Reference Units (IRU), Three-Axis Magnetometers (TAM), Coarse Sun Sensors (CSS), Magnetic Torquer Bars (MTB), Reaction Wheel Assemblies (RWA), Engine Valve Drivers (EVD) and thrusters. The ACE is comprised of an 80C86 processor, DC-DC converters, and actuator and sensor interface electronics. The ACE processor formats raw sensor data, decodes commands and contains Safe Hold flight software. The ACE transmits the sensor data over a 1773 fiber optics data bus to the ACS processor to be used by the ACS software and down-linked in telemetry. The flight software for initialization, attitude determination and control, momentum management, ephemeris generation, solar array commanding, High Gain Antenna (HGA) commanding, mode management and Fault Detection and Correction (FDC) are implemented in the ACS Processor. The FDC software provides tolerance of a single point failure with minimal interruption to science data gathering. The computed control torques are sent back to the ACE, which relays the appropriate

commands to the actuators. The TRMM ACS operates at a 2 Hz control rate while in Mission Mode. All TRMM ACS components are fully redundant and cross-strapped with the exception of the MTBs which have redundant windings that are not cross-strapped.
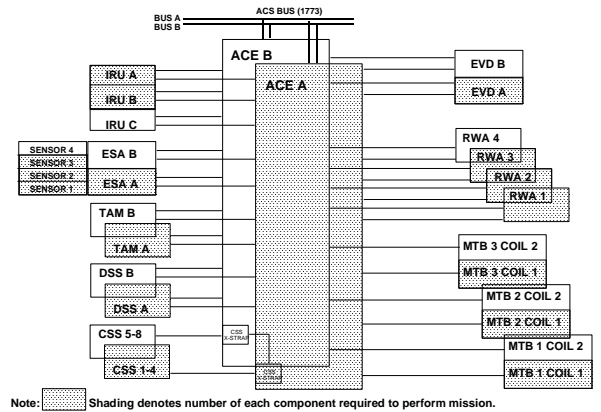

Figure 3: ACS Architecture

The ACS Mission Mode utilizes a static ESA, two DSS's and IRUs for attitude sensing. The ESA provides roll (X) and pitch (Y) axis attitude error measurements. Yaw (Z) position is determined with DSS updates and propagated between updates using gyro output. Four RWAs arranged in a pyramid configuration are used for control. The TAM and three MTBs are used for momentum management. A simple Proportional-Integral-Differential (PID) controller is used in Mission Mode, as shown in Figures 4 and 5.
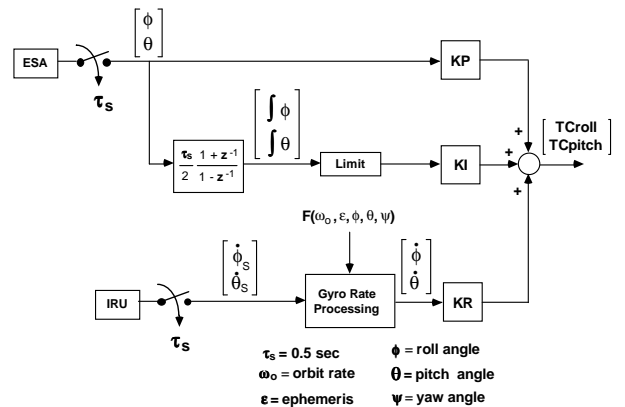

Figure 4: Mission Mode Roll / Pitch Controller
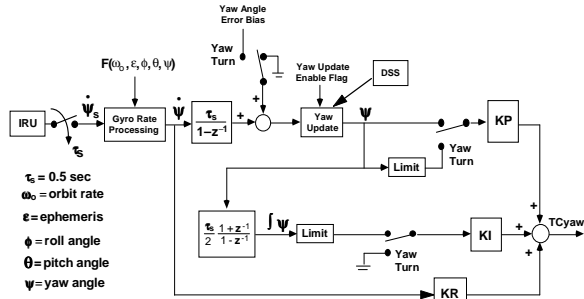
Figure 5: Mission Mode Yaw Controller

The ESA used on TRMM is an infrared horizon sensor with no moving parts. The ESA independently views segments of the horizon in the centers of the North-East, North-West, South-East, and South-West quadrants. Each quadrant contains four detectors, three of which are nominally in view of the Earth limb. The fourth detector, known as the S detector, is nominally in view of cold space and provides a space radiation measurement.

Each of the DSS's has a pair of heads mounted orthogonally to provide two axes of information. Each head senses the Sun angle in a single axis over a 96^0 Field Of View (FOV) about the head bore-sight axis. Twice an orbit, the DSS readings are compared to an ephemeris-based expected reading to provide an attitude reference for the yaw axis gyro as well as a new yaw gyro bias. One DSS looks in a forward (+X) direction and another points in the aft (-X) direction, as shown in Figure 6. The bore-sight orientations were chosen so as to maximize the time during which DSS data was available.
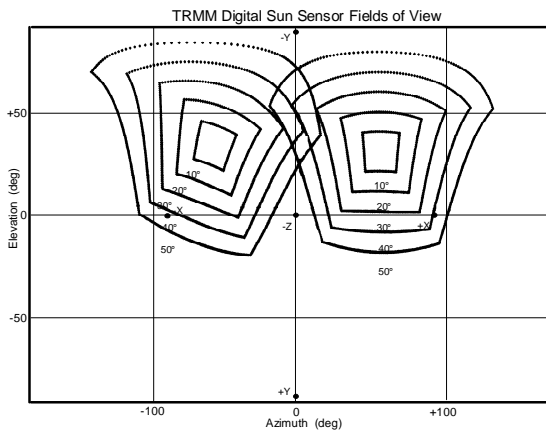
**Figure 6: TRMM DSS Field of View**

On-Orbit Checkout

On-orbit checkout of the TRMM Mission Mode uncovered two unexpected performance features. Both anomalies were dealt with by uploading new table values in the ACS flight software.

Soon after launch, a significant inconsistency between the output of the DSS's was found. Consequently, each on-board yaw attitude update resulted in a significant attitude change. The yaw measurement from one DSS was inconsistent with the previous update, from the other DSS. The spacecraft compensated by maneuvering to null the new yaw measurement and computing a new gyro bias, based on spacecraft attitude motion assumed to be equal to the difference between the two DSS yaw measurements. The new gyro bias was used to control the spacecraft until the next yaw update, resulting in a larger update.

The cycle of DSS and gyro bias correction on-board resulted in the spacecraft attitude developing the pattern shown in Figure 7. The ground solution is obtained by gyro propagation of the epoch attitude from a batch least-squares computation using a full orbit's sensor data. Batch processing of this amount of data results in an attitude that uses all of the data and therefore is more accurate than an instantaneous sensor measurement.

The ACS drives the on-board computed attitude errors to zero. The On-Board Computer (OBC) attitude therefore shows constant, near zero attitudes except at each yaw update. When a new inconsistent DSS measurement shows a yaw deviation, the spacecraft maneuvers to remove it. This results in a brief spike in the OBC yaw attitude.
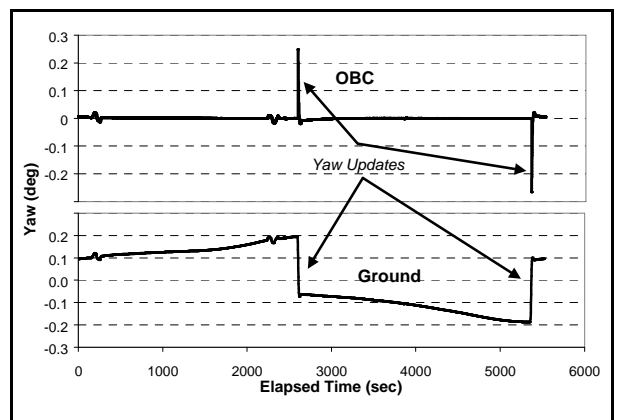
Figure 7: Pre-calibration Yaw Attitude

The spikes in the yaw position were found to be caused by a misalignment of the two DSS heads with respect to each other. The flight software assumed that the DSS heads would be mounted orthogonal to each other, when in fact a review of alignment records indicated that the heads were only mounted orthogonal to within approximately 0.2^0. The effect of this misalignment on attitude performance was minimized post-launch through sensor calibration, as described in the next section.

Another unexpected spike in position error was found to occur in roll and pitch during periods of time when the Sun was in one the ESA quadrant's FOV. The top plot in Figure 8 shows spikes in the pitch position error which correspond to Sun passage through one of the ESA quadrant's FOV. It was determined that these spikes were caused by the on-board ESA processing. The S detector output is filtered by the on-board software. When the Sun is predicted to intrude into a quadrant FOV, that quadrant is not used in attitude computations and the S detector for that quadrant is not filtered. When the Sun is predicted to leave the quadrant FOV, it is then again used in attitude computations and filtering of the S detector resumes.
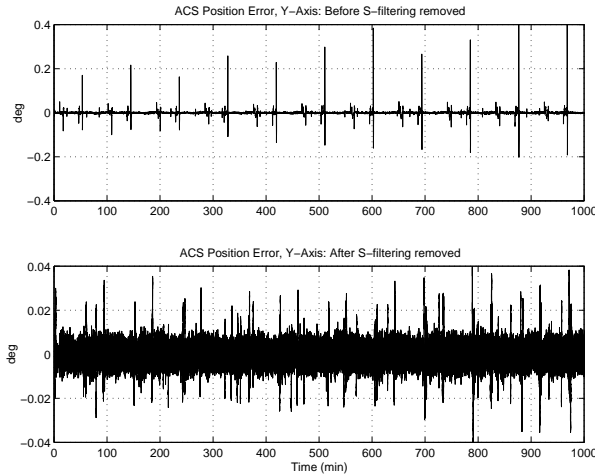
Figure 8: ACS Position Error

The spikes in position error resulted from an error in the on-board algorithm which did not reset the S filter properly when it was turned back on. The spikes are the dynamical response of the filter as it settles after this sudden jump in data. The bottom plot in Figure 8 illustrates the position error with S filtering turned off during a period of time when the Sun passes through the same ESA quadrant FOV. It can be seen that the removal of the S filter has greatly minimized the effect of spikes due to Sun intrusion. A flight software change

could be made to correct the S filter initialization; however, the performance with the S filter turned off was deemed to be adequate.

Sensor Calibration and Attitude Validation

The TRMM attitude sensors were calibrated after launch in order to improve on-orbit performance. The relative alignment of the ESA and the two DSS's were determined to improve attitude consistency. Changes in the DSS transfer function coefficients were determined in order to compensate for the non-orthogonality of the DSS heads. The gyros were calibrated to improve the targeting accuracy of slew maneuvers. Because the magnetometers are only used for attitude determination in a contingency mode, their calibration is not described here.

Alignment Calibration: Alignment calibration is performed on orbit to insure that the computed attitude is consistent, regardless of which sensors are used as input and regardless of the relative amounts of data received from each sensor. For TRMM, on-board roll and pitch were taken directly from the ESA while yaw was taken from the two DSS's. Ground computation of attitude was performed by a batch-least squares algorithm using input from both of the DSS's, the ESA and the gyros.

A portion of the attitude inconsistencies was found to have been caused by misalignment of the DSS's and the ESA relative to each other. The effect of the misalignment of the DSS's was removed by determining a misalignment matrix, **M**, and applying it to the raw DSS vectors before applying the nominal alignment transformation, **N**, to transform these vectors from the sensor to the body frame.

$$\hat{O}_{body} = N_{\text{nominal\_to\_body}} \ M_{\text{true\_to\_nominal}} \hat{O}_{observed} \quad (1)$$

The misalignment matrices, M, were determined using two algorithms that gave similar results. Both used all sensor data in a batch least-squares algorithm to minimize a Wahba loss function:

$$\mathcal{L} = \sum_{t,i} W_i \left[A_t \hat{R}_{t,i} - N_i M_i \hat{O}_{t,i} \right]^2 \quad (2)$$

where the A_t is the attitude at time t, N_I, $\mathbf{M}_I$, and W_I the nominal alignment, misalignment matrix and weight for sensor I, and $\mathbf{O}_{t,I}$ and $R_{t,I}$ are observation and reference vectors from sensor I at time t.

The misalignment of the ESA was parameterized in terms of penetration angle biases. These biases are the difference from nominal that the Earth horizon penetrates into individual single quadrants when the pitch and roll are zero. Differences between penetration angle biases on opposite quadrants are equivalent to misalignment angles.

The first algorithm minimized this loss function with respect to a state vector including an epoch attitude, gyro biases, and misalignment parameters. The second algorithm minimized the same loss function with respect to only the epoch attitude and gyro biases (keeping a identity misalignment matrices for all three sensors and zero penetration biases for the ESA) to produce a reference attitude and gyro biases. A second step was then used to minimize the loss function (using the gyro-propagated attitude from the first step) with respect to the misalignment parameters.

Both of these algorithms give relative alignments because a misalignment corresponding to the rotation of all of the sensors together is inherently unobservable. Before launch it had been decided that DSS-2 would be used as the reference sensor. The specific misalignments were to be determined so that the misalignment of DSS-2 would be identity. This choice was made because mechanical analysis indicated that DSS-2 would be less likely to shift at launch than DSS-1. The second cause of the attitude behavior shown in Figure 7 was due to the two heads of each DSS not being mounted orthogonal to each other. Because this misalignment was smaller for DSS-1, the reference was changed to DSS-1.

Using $\mathbf{M}_{DSS-1} = \mathbf{I}$, the misalignment matrices of DSS-2 and penetration angle biases of the ESA were found to be:

$$M_{DSS-2} = \begin{bmatrix} 999.996 & -1.98736 & -1.99437 \\ 1.99280 & 999.994 & 2.72920 \\ 1.98893 & -2.73316 & 999.994 \end{bmatrix} \times 10^{-3}$$

(3)

$$b_{ESA} = \begin{bmatrix} -0.1574 \\ 0.04635 \\ -0.09414 \\ -.05382 \end{bmatrix} \text{degrees}$$

Figure 9 shows the root-mean-square (RMS) differences between OBC and ground batch least-squares attitudes computed for the first several months of the mission. Because the ground solutions use all of the data, including gyro data, they are more accurate than the OBC attitudes and this figure can be considered to be a plot of OBC attitude errors. The six vertical dotted lines are drawn (on this and on the two subsequent figures) at the times when TRMM had 180^0 yaw maneuvers to change its orientation with respect to the Sun. As can be seen from the figure, uplink of the new alignments significantly reduced the OBC attitude error.
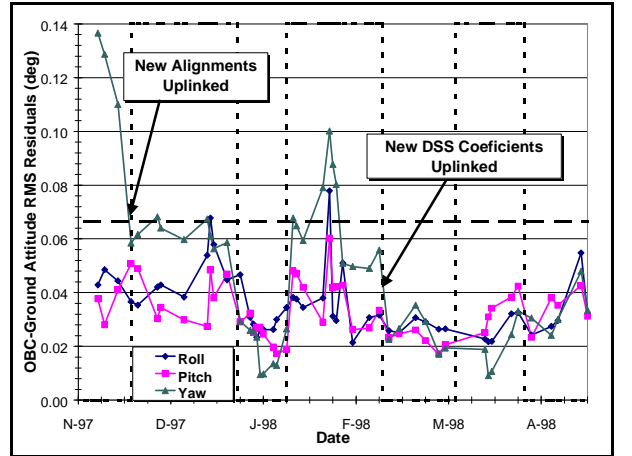

Figure 9: RMS Attitude Error

The horizontal dashed line in Figure 9 represents the required (1σ) TRMM attitude accuracy.

Figure 10 shows the effect of calibration on the size of the yaw update throughout the early mission. Uplink of the new alignments significantly decreased the size of the yaw update.
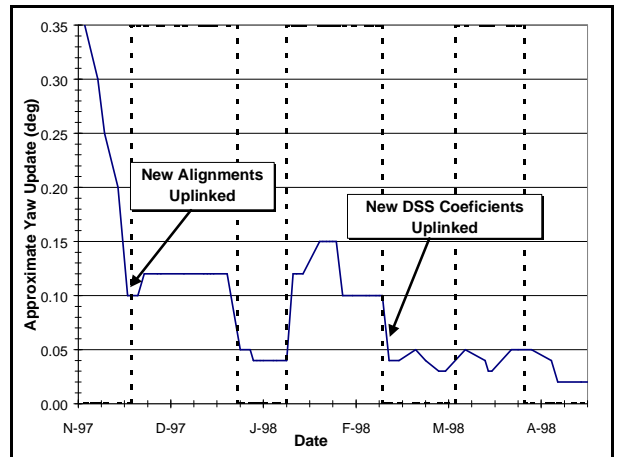

Figure 10: Yaw Update

DSS Transfer Function Calibration: A major cause of the attitude inconsistency resulting in the behavior shown in the figures above was non-orthogonality of the DSS heads. Each DSS contains two heads that measure angles in two, nominally orthogonal, directions. These two angles, α and β, are converted to an observed Sun unit vector in the sensor frame by:

$$\hat{O}_{Sun} = \begin{bmatrix} \tan\alpha \\ \tan\beta \\ 1 \end{bmatrix} \left(\tan^2\alpha + \tan^2\beta + 1\right)^{-1/2} \quad (4)$$

Analysis of the large attitude changes at each yaw update led to an investigation of the prelaunch head mounting geometry. The α and β heads of both sensors (especially DSS-2) were mounted at an angle with significant misalignments. If the orientation of the β head is represented as a 2-3-1 Euler sequence, the rotation angles of DSS-1 were 0.044, -0.008, and 0.067 deg while those of DSS-2 were 0.206, 0.061, and 0.182 deg.

Unfortunately, the on-board attitude software, the ground attitude determination software, and the sensor calibration software were not designed to determine or use non-orthogonal misalignment matrices.

Three factors existed that allowed for a relatively simple and effective compensation for the DSS head non-orthogonality. The DSS data was only used to update yaw attitudes at one specific value of α in each DSS, the calibration software was capable of determining new transfer function coefficients for the DSS's, and the on-board software was capable of using these new coefficients.

The DSS α and β observations are generated from raw output of the two heads, N_α and N_β, by:

$$\alpha = \tan^{-1}\left[\begin{array}{l} a_1 + a_2 N_\alpha + a_3 \sin(a_4 N_\alpha + a_5) \\ + a_6 \sin(a_7 N_\alpha + a_8) \end{array}\right] + a_9$$

$$\beta = \tan^{-1}\left[\begin{array}{l} b_1 + b_2 N_\beta + b_3 \sin(b_4 N_\beta + b_5) \\ + b_6 \sin(b_7 N_\beta + b_8) \end{array}\right] + b_9$$

$$(5)$$

Non-orthogonality of the DSS heads resulted in a formal dependence of transfer function coefficients on the position of the Sun relative to the sensor boresight.

It was suggested that this dependence could be compensated using new values of the coefficients that minimized errors at the time of each yaw update. To eliminate the dependence of the a-coefficients on the position of the Sun, the α axis of each sensor was taken as its reference axis. Because the yaw updates always occur when the Sun vector intersected the XY body plane, minimum error β values were obtained using b-coefficients given by:

$$b_1' = cb_1 + d$$
$$b_i' = cb_i \quad i = 2,3,6$$

$$(6)$$

Based on pre-launch head misalignments, the resulting values of *c* and *d* were 1.000047 and 0.000085 for DSS-1 and 0.999977 and 0.000053 for DSS-2.

As can be seen in Figures 9 and 10, the use of these new coefficients (after February 27, 1998) decreased both the attitude error and size of the yaw update. An interesting, but unexplained, observation is that before uplink of these coefficients the yaw attitude was more accurate, and the yaw updates smaller, in the +X forward configuration than in the –X forward configuration. After uplink of the coefficients the values were small in both configurations.

Gyro Calibration: Calibration of spacecraft gyros does not affect the accuracy of spacecraft attitudes as long as the attitude solution method contains gyro biases in its state vector and the spacecraft rates are approximately constant as they are in Mission Mode. Gyro calibration is performed in order to improve the accuracy of maneuver targeting.

Raw gyro rates, ω_0, are converted to adjusted rates by:

$$\vec{\omega} = G\vec{\omega}_0 + \vec{b}$$
$$G = MS$$

$$(7)$$

where *M* is a true normalized misalignment matrix, *S* a diagonal scale factor matrix, *G* the product of the two (not orthonormal) and *b* a bias vector. Using an a priori values of $G = I$ and assuming ω_0 is nearly constant:

$$\vec{\omega} = \vec{\omega}_0 + \vec{b}' \quad \text{where}$$
$$\vec{b}' = \vec{b} + (MS - I)\vec{\omega}_0$$

$$(8)$$

where $\vec{b}'$ is the *solved for* bias vector.

During attitude maneuvers, rates are not constant so the attitude change during a maneuver from t_0 to t depends on the misalignment matrix, scale factors, and bias vector.

Gyro misalignments, scale factors, and biases were determined using a transition-matrix version[2] of the Davenport method[3,4]. This method requires data from at least four separate intervals in which the integrated rate vectors are linearly independent. For TRMM, an interval in normal Mission Mode, an interval during a 180^0 yaw maneuver, and intervals during CERES and Precipitation Radar (PR) calibration maneuvers were used.

To use the Davenport algorithm, reference attitudes at times immediately before and after each calibration period were computed using data from constant rate periods before and after each maneuver. Because TRMM rates were constant during these periods, accurate reference attitudes could be obtained at each of these times. The attitude at the end of each calibration period depends not only on the attitude at the start but also on the gyro misalignments, scale factors, and biases. Values for these parameters were found that minimized the differences between reference attitudes and propagated attitudes at the end of each interval. The propagated attitudes were computed by propagation of the reference attitude at the start of each interval using gyro data adjusted with the misalignments, scale factors and biases.

The results of the calibration were:

$$G = \begin{bmatrix} 1.000443 & -1.01300 \times 10^{-3} & 6.75235 \times 10^{-4} \\ 7.63599 \times 10^{-4} & 1.00053 & -2.1629 \times 10^{-3} \\ 9.41394 \times 10^{-4} & 1.6831 \times 10^{-3} & 1.00088 \end{bmatrix}$$

(9)

$$\vec{b} = \begin{bmatrix} -1.549155 \\ 1.978161 \\ 0.7820254 \end{bmatrix} \times 10^{-4} \text{ deg/sec}$$

The calibration success was evident in two ways. Targeting of the 180^0 yaw maneuvers became significantly more accurate in all three axes. The error in yaw, pitch, and roll attitudes after a 180^0 yaw maneuver are shown in Table 2. This table gives figures for the same yaw maneuver propagated using the precalibration and postcalibration gyro parameters. Note that, probably due to misalignment, the roll attitude was significantly in error before calibration, and

that this error was dramatically reduced by the calibration.

Table 2: Yaw Maneuver Attitude Error (deg)

Attitude Component	Precalibration Error	Postcalibration Error
Yaw	-0.096830	-0.044520
Pitch	0.010712	0.005767
Roll	0.248440	-0.005775

The increase in targeting accuracy is especially important for TRMM because the on-board attitude determination accepts yaw input only twice each orbit. A significant period might therefore elapse between the end of a yaw maneuver and the next yaw attitude update. During this period TRMM would have significant attitude error.

If the calibration parameters are correct, the bias vector solved for using the normal attitude determination methods should be independent of the (nearly constant) rates. TRMM pitches at ±1 revolution per orbit (RPO) depending on whether it is flying +X forward or –X forward. Differences between the apparent gyro biases computed while it rotates at either + or –1 RPO shows the calibration accuracy. A plot of gyro biases during the first 5 months of operation is shown in Figure 11. The variation in gyro bias depending on TRMM orientation is clearly evident before the uplink of the gyro calibration parameters. For the first maneuver (on March 21, 1998) after these parameters were applied the computed gyro biases became nearly independent of TRMM orientation.
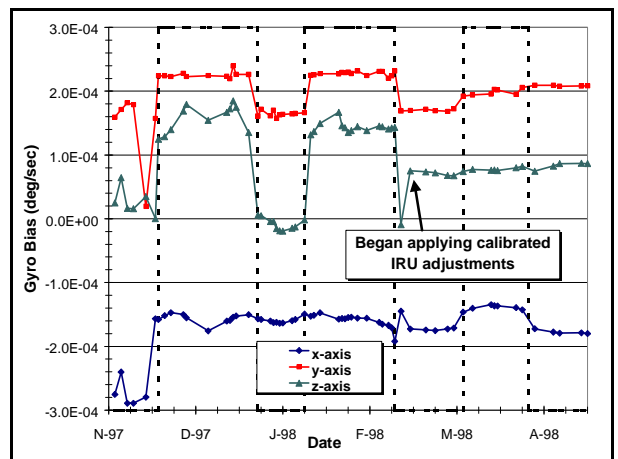
Figure 11: Ground Determined Gyro Biases

On-orbit Performance: The attitude performance of TRMM Mission Mode is summarized in Table 3.

In this table three measures of performance are displayed: attitude accuracy, yaw update, and the standard deviation of the gyro bias. The attitude accuracy is the average over the period of RMS differences between batch least-squares ground attitudes and the OBC attitudes. Each RMS difference is taken over at least a full orbit of data. The yaw updates are an average of the attitude change that occurred each time the yaw attitude was updated on-board. The standard deviations of gyro biases show how stable the biases were during each period.

The periods used for performance evaluation were
- Precalibration: Launch to December 11 (before any calibration parameters were uplinked)
- Calibration 1: December 11 to February 28 (after alignment calibration values were uplinked)
- Postcalibration: All of March and April (period after the DSS FOV coefficients and gyro calibration parameters were uplinked)

For the gyro bias parameters only two periods are used corresponding to the second and third of those used for the other parameters.

Table 3: TRMM Mission Mode Attitude Performance

| Parameter	Axis	Pre-calibration	Calibration-1	Post-calibration
Attitude Accuracy (deg)	Roll	0.045	0.038	0.029
	Pitch	0.036	0.035	0.030
	Yaw	0.130	0.051	0.026
Yaw Update (deg)		0.24	0.10	0.04
Gyro Bias Standard Deviation (deg/hour)	X	0.0312		0.0668
	Y	0.1046		0.0579
	Z	0.2675		0.0214

Calibration of the attitude sensors and gyros significantly improved TRMM attitude performance. Before calibration the yaw attitude did not meet mission requirements while after calibration it fell well within requirements. The mitigation of the unexpected yaw updates was particularly gratifying. The decrease in the size of yaw updates is easily seen by comparing the precalibration ground and on-board attitudes in Figure 7

with the corresponding postcalibration values in Figure 12.
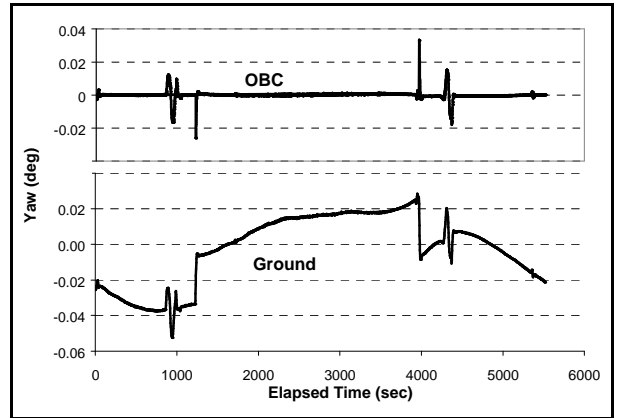
Figure 12: Post-calibration Yaw Attitude

The postcalibration attitude error for TRMM, over a full orbit, is shown in Figure 13.
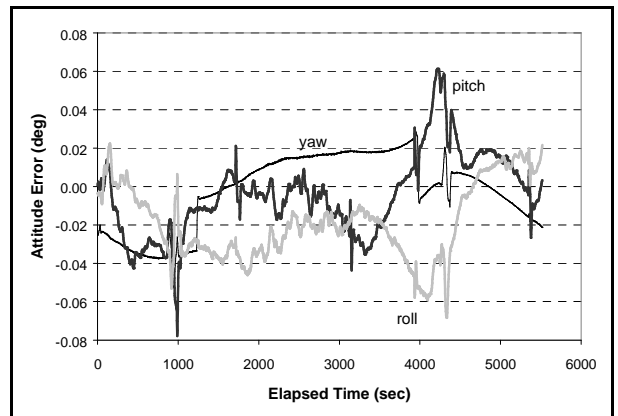
Figure 13: Post-calibration TRMM Attitude

Conclusion

The on-orbit performance of the TRMM ACS has been presented along with the mission level requirements. Flight data results show that the TRMM ACS is meeting all of the imposed requirements after sensor calibration. Lessons learned were realized during on-orbit checkout and sensor calibration.

The obvious lesson learned deals with the nonorthogonal mounting of the DSS heads. This lesson learned deals with the importance of communication between engineers and the importance of allowing flexibility in the ACS flight software. More thorough communication between the ACS and Mechanical engineers could have prevented a misunderstanding of

the importance of mounting the heads orthogonal with high precision. More attention during integration to the detail of the alignment measurement summary on the part of the ACS team could have identified the problem prior to launch. Finally, the ACS flight software should have been designed with the flexibility to accommodate misalignments of each head rather than each DSS. The flight software should have been designed to have alignment matrices or coefficients that could be uploaded to accommodate misalignments between heads.

Another lesson learned deals with the importance of sensor model fidelity. The post launch removal of the S filter in ESA processing could have been avoided if the thermal dependence of the ESA had been modeled in simulations. The problem with the S filter initial condition when switching from 3 back to 4 quadrant processing was not uncovered because a non-thermally dependent ESA model was used in all simulations and flight software qualification tests. Alternatively, a high fidelity stimulator of the ESA capable of stimulating 3 and 4 quadrant processing could have uncovered the problem during test.

Acknowledgements

References

1. "TRMM Attitude Control System Specification," TRMM-712-046, January 31, 1992.

2. G. Natanson, "A Transition Matrix Approach to the Davenport Gyro Calibration Scheme," *Proceedings of the 13th International Symposium on Space Flight Dynamics,* NASA Conference Publication AAS 98-335, Greenbelt, MD, May 1998, pp. 373–388.

3. P. Davenport, *In-flight Calibration of Gyros*, Goddard Space Flight Center, Spring 1976

4. J. Keat, *Gyro Calibration Analysis for the High Energy Astronomy Observatory-A (HEAO-A)*, CSC/TM-77/6082, prepared by Computer Sciences Corporation, June 1977